ORIGINAL RESEARCH PAPER

Narrow band based and broadband derived vegetation indices using Sentinel-2 Imagery to estimate vegetation biomass

A.B. Imran[1], K. Khan[2,*], N. Ali[3], N. Ahmad[4], A.Ali[4], K. Shah[4]

[1]Department of Forestry and Range Management, PMAS Arid Agriculture University, Rawalpindi, Pakistan
[2]Institute of Environmental Science and Engineering, National University of Science and Technology, Pakistan
[3]Department of Forestry and Wildlife Management, University of Haripur, Pakistan
[4]Ministry of Forestry, Environment and Wildlife, Khyber Pukhtunkhwa, Pakistan

ARTICLE INFO

ABSTRACT

Forest's ecosystem is one of the most important carbon sink of the terrestrial ecosystem. Remote sensing technology provides robust techniques to estimate biomass and solve challenges in forest resource assessment. The present study explored the potential of Sentinel-2 bands to estimate biomass and comparatively analyzed of red-edge band based and broadband derived vegetation indices. Broadband indices include normalized difference vegetation index, modified simple ratio and atmospherically resistant VI. Whereas, red-edge band indices include two red-edge normalized difference vegetation index and sentinel-2 red-edge position. Results showed that red-edge band derived spectral indices have performed better than the Broadband indices. The coefficient of correlation for normalized difference vegetation index, modified simple ratio and atmospherically resistant-VI was 0.51, 0.44 and 0.31 respectively, On the other hand, red-edge band indices showed higher correlation of R^2 0.62, 0.64 and 0.55, respectively. Similarly, in stepwise regression red-edge normalized difference vegetation index (using band 6) was selected in final model (as overall R^2 of the model was 0.60) while all other indices were removed because they have non-significant relationship with the biomass. Accuracy assessment shown the red-edge index has highest R^2 (0.64) and least error of (31.29 t/ha) and therefore the study concluded that narrowband indices performed better to estimate biomass and thus final model contained only red-edge index to predict biomass over the study area. The study suggests that more in-depth research should be conducted to explore further properties of red-edge indices for vegetation parameters prediction.

NUMBER OF REFERENCES

32

NUMBER OF FIGURES

5

NUMBER OF TABLES

4

*Corresponding Author:
Email: naveed.iese.nust@gmail.com
Phone: +92 309 4032077
Fax: +92 51 9290459

Note: Discussion period for this manuscript open until April 1, 2020 on GJESM website at the "Show Article.

INTRODUCTION

Forest's ecosystem is one of the most important carbon sink of the terrestrial ecosystem. Carbon stocks required intensive in-situ forest inventory which is considered the most accurate method, however it has many limitations such as it is expensive, time consuming, destructive, applicable for only a small sample of trees and small spatial coverage (Mohren *et al.,* 2012). Remote sensing provides robust techniques to estimate biomass and solve challenges in forest resource assessment (Mundava *et al.,* 2014: Dusseux *et al.,* 2015; Karakoç *et al.,* 2019). Remote-sensing techniques can provide information at a wide range of spatial and temporal scales, wall-to-wall coverage, frequent 'revisit' of the area, and use as historic archives of data. Nevertheless, field-based biomass estimations are absolutely essential for remote sensing methodologies for calibrating models and verifying results (Adam *et al.,* 2010). Several studies have been conducted to estimate the forest biomass using the data of remote sensing with the integration of the field data (May *et al.,* 2010; Dusseux *et al.,* 2015). Sentinel-2 is the state-of-the-art sensor of European Space Agency (ESA), was launched in 2015 which comprised 13 bands extending from visible, near infrared, shortwave infrared with a high spatial resolution (10 to 60 m range) (Gholizadeh *et al.,* 2016). Sentinel-2 has immense potential to estimate various vegetation parameters such as Leaf Area Index, chlorophyll and nitrogen, biophysical parameters and Red-Edge Position (Frampton *et al.,* 2013; Richter *et al.,* 2012; Clevers and Gitelson, 2013; Verrelst *et al.,* 2013; Delegido *et al.,* 2013). The present study explored spectral indices computed from Sentinel-2 product. The broadband indices derived from Sentinel-2 images include Normalized Difference Vegetation Index, Modified Simple Ratio and Atmospherically Resistant Vegetation Index (ARVI). Of course, the most used vegetation index is the Normalized Difference Vegetation Index (NDVI) which is normally applied to analyze vegetation and its temporal changes on local and regional scales (Ali *et al.,* 2018). Modified Simple Ratio (MSR) is the improved form of Ratio Vegetation Index (RVI) which is the most basic index applied in vegetation analysis and monitoring (Calvão and Palmeirim, 2011). The atmospheric effects are normally minimized by ARVI

by using reflectance in Red, Blue and NIR regions. The parameters of atmospheric scattering (aerosols and ozone) are difficult to quantify but its influence can be decreased by ARVI (Wang *et al.,* 2017). Therefore, this study also used ARVI in addition to NDVI and MSR with the expectation that this index may have good potential for biomass estimation. Further, in order to utilize narrowband information to estimate biomass, Red-Edge band based indices were also computed (Karakoç *et al.,* 2019). Based on literature, three Red-Edge indices were selected and compared with broadband indices. Out of these three indices, two Red-edge NDVI using Band 04 (Red) and Band 06 and 07 (the Red-edge bands). While the third was Sentinel-2 Red-Edge Position (S2REP) which shows the difference between maximum absorption in Red portion and highest reflectance in NIR portion. Red-Edge (RE) denoted the spectral area of slope of reflectance of forest canopy between 680-740 nm and thus uses an important indicator to investigate health of the plants and pigmentation (Clevers and Gitelson, 2013). Besides this Red-Edge Inflation Point (REIP) is wavelength of maximum slope (the first derivative) between 680-740 nanometers (nm) region and scattering due to atmosphere and soil substrate are minimum in this region while predicting vegetation properties (Cho and Skidmore, 2006; 2008). S2REP is very useful to quantify chlorophyll contents, and chlorophyll contents in green leaves which offered important information. Further, this index is very useful to differentiate leaf internal scattering and indicate strong Chlorophyll absorption. The slope of S2REP is an indication of growth period and nutrient contents because increased amount of chlorophyll. Different techniques have been used for abstraction of SEREP parameters based on Sentinel-2 spectral data, among the most widely used methods is vegetation indices derived from Red-Edges Indices. Presently, Sentinel-2 may be considered as one of the four satellites that are equipped with RE bands composition and other three are WorldView-2, WorldView-2 and RapidEye (Drusch *et al.,* 2012; Kross *et al.,* 2015; Karlson *et al.,* 2016; Asadzadeh *et al.,* 2016). Therefore, this study is specifically focused on the vegetation indices computed from Red-Edge bands of sentinel-2 and compared them with broadband indices. This study has been carried out in Muzafferabad, Pakistan in 2019.

MATERIALS AND METHODS

Study area

The study area of the present research was Muzafferabad, which is capital city of Azad Jammu and Kashmir state of Pakistan (Fig. 1). The study area is situated at the convergence of two main rivers namely Jehlum and Neelam that are originated from Indian Occupied Kashmir area. The climate of Muzafferabad is Moist Temperate where 36°C and 23°C are the mean minimum and maximum temperature in July respectively and the weather becomes colder and colder in the following month and reached to 16°C (maximum) and 3°C (minimum) temperature in January. The mean annual precipitation was also observed high i.e 1511 mm and areas are located at the north of the study area are comparatively colder than the southern regions. Regarding agriculture, people of the Muzafferabad grow miaze, wheat, rice, pulses, vegetables on the contours and terraces developed in mountains. Further, the study area is also a focal point for variety of fruits such as apple, pear, plum, apricot and walnut. Agriculture mainly dependent on rain waters and small tributaries linked with perennial rivers as there is no extensive canal system. The study area is covered with 59 percent of forest cover of district area and forests are considered as one of major source of income for local communities. Major tree species include Cedrus deodara, Pinus wallichiana, Abies pindrow, Picea smithiana, Pinus roxburghii, Juglan regia, Maple, Poplus cilliata, Salix, Quercus species (ERRA, 2007).

Methods

The research study was carried out by estimating biomass through field inventory and remote sensing. First, field Inventory for this present study comprised of total 65 circular sample plots of 0.1 ha area were randomly laid out in the forest and all the trees inside the circle were enumerated (Molto et al., 2013). Diameter at breast height (DBH) and height of all trees in a sample plot were measured for Above ground biomass determination using Eq. 1 (Schoene, 2002; Fukuda et al., 2003). Volume (m^3) was calculated from DBH and height values. Whereas Basic wood density (kg/m^3) and Biomass expansion factor (BEF) were taken from literature of Pakistan Forest Institute, Pakistan. Mostly remote sensing research of biomass estimation used BWD and BEF from literature.

$$Biomass = V \times BWD \times BEF \qquad (1)$$

Where, V = timber volume in m^3
BWD = Basic wood density in kg/m^3
BEF = Biomass expansion Factor.

Secondly, biomass values were converted carbon stocks and as per intergovernmental panel on climate change standards half of the dry biomass is carbon stock and finally carbon stocks were converted into carbon credits for carbon trading. Thus the dry biomass can be converted to carbon stock by multiplying it
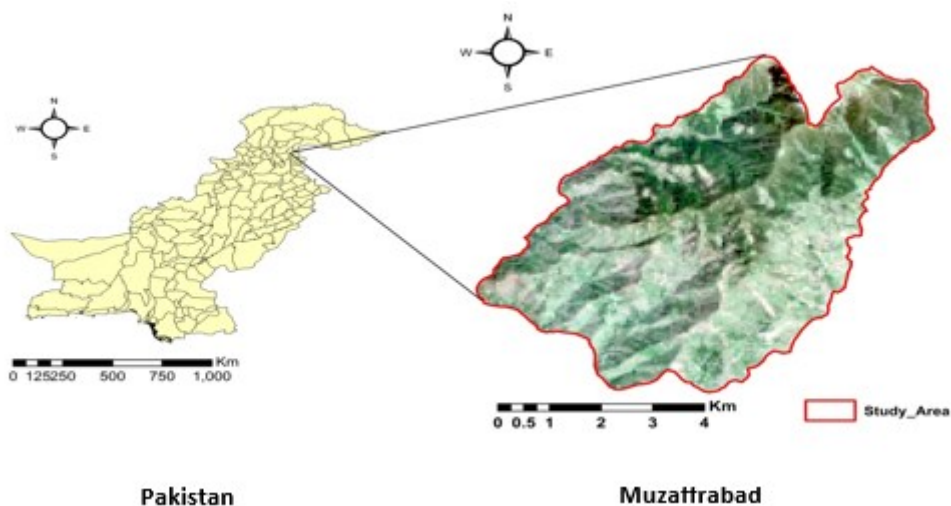

Fig. 1: Geographic location of the Study area in Muzafferabad, the capital city of Azad Jammu and Kashmir state of Pakistan

with 0.47 (Paustian *et al.,* 2006). Therefore, forests acts as carbon sinks for greenhouses emissions. Estimated AGB from in-situ field data has been summarized in supplementary table (Table S1). Above ground biomass (AGB) attributes data were imported into ArcGIS 10.3 and shape file and this AGB values were then correlated with computed vegetation indices. Secondly, in the present study Sentinel-2 was used to overcome limitation of resolution that was previously provided by other open source sensors (e.g Landsat-8) (Gascon and Berger, 2007). The image was downloaded from Copernicus Sentinel Scientific Data Hub for Muzafferabad forests area for the specific time and location. The sentinel-2 product was registered in ellipsoid World Geodetic System (WGS) 1984 with Universal Transverse Mercator (UTM) projection system. Image preprocessing was the first step before it used for the biomass estimation purpose (Roy *et al.,* 2016). The purpose was to avoid effects of atmospheric scattering or cloud cover shadows, to aid visual interpretation and to extract plenty of information from remotely sensed images. Pre-processing includes radiometric, geometric and terrain correction respectively Sentinel 2 images were preprocessed in SNAP Tool Box (Egbers, 2016; Martins *et al.,* 2017). Sen2Cor is a plugin SNAP tool box for atmospheric correction. Level 1C product "Top of the atmosphere (ToA)" was converted into atmospherically corrected level 2A product. The processing of Level 1C product include cloud detection, scene classification, Aerosol Optical thickness and water vapor contents, all these were processed by Sen2cor processor to obtain Bottom of atmosphere conversion (BoA), (Louis *et al.,* 2016; Martins *et al.,* 2017). Sub setting of image was done

for area of interest where forest inventory was conducted. Further, different vegetation indices were computed using SNAP Tool box (Chrysafis *et al.* 2017; Ali *et al.,* 2018). Mostly the broadband indices undergo various mathematical operations using two bands (in Red and Near Infrared region), which expressed vegetation cover from other objects. The lower values show area of less or no vegetation while the increasing values shows higher vegetation density. Negative values indicated no vegetation such as water bodies. However, NDVI has few limitations because its values are influenced by reflectance from soils and signal scattering by cloud cover and atmospheric particles. Moreover, saturation issues are reported for broadband indices (NDVI) in higher biomass areas. As depicted in Table 1, first five vegetation indices were computed using photosynthetically important bands in Sentinel-2 product, band ratio were developed using Band 2 (Blue band), Band 4 (red band), Band 6 (RE band 6), Band 7 (RE band 7) and Band 8A (Near Infrared band). Whereas S2REP index was computed by using the equation given in Table 1 which used difference of reflectance between chlorophyll absorption at red band and reflection at infrared regions. AGB shape file created via ArcGIS 10.3 was overlaid on corresponding vegetation indices of Sentinel-2 image. The masked pixels values were extracted for all the indices and were converted into excel sheets.

Statistical analysis

Statistical analysis include correlation, simple linear regression and stepwise linear regression were developed. The independent variable was spectral index/indices computed from Sentinel-2

Table 1: Broadband and narrowband vegetation indices for sentinel-2

Indices	Sentinel-2 Band Combination	References
	Braodband vIs	
Normalized difference vegetation index (NDVI)	(B8- B4) ÷ (B8 + B4)	Rouse *et al.,* 1973
Atmospherically Resistant Vegetation Index (ARVI)	$(\rho B8 - \rho B4 - (\rho B2 - \rho B4))/(\rho B8 + \rho B4 - (\rho B2 - \rho B4))$	Kaufman and Tanre, 1992
Modified simple ratio (MSR)	$((\rho B8/\rho B4 - 1)/ \sqrt{((\rho B8/\rho B4) + 1)})$	Chen, 1996
	Narrowband vIs	
Red-Edge NDVI-1	(B6 −B4)/ (B6+B4)	Adan, 2017
Red-Edge NDVI-2	(B −B4)/ (B7+B4)	Adan, 2017
Sentinel RE position (S2REP)	$705 + 35 \times \dfrac{\frac{\rho783 + \rho665}{2} - \rho705}{\rho740 - \rho705}$	Adan, 2017

image and dependent variable was AGB field data. Model selection was based on value of coefficient of correlation and root mean square error (RMSE). Best model for biomass prediction have least RMSE and highest coefficient of correlation.

RESULTS AND DISCUSSION

Broadband indices
NDVI and AGB

The scatter plot between AGB values from field data and NDVI values derived from image has been shown in the Fig. 2a. The coefficient of correlation was 0.51 which mean that 51% of field data have been explained by the NDVI-based model while 49% of the data are not explained by this model. However NDVI is a proxy data and this much coefficient of correlation is considered good. The correlation of NDVI was greater than (MSR, ARVI). The Fig. 4a showed that higher forest density was found at North moving towards south and eastern part is comparatively less. The Fig. 4a showed range of NDVI between 0.06 and 0.99; the positive values (0.99 or less) showed vegetation cover while the 0.06 values show no or less vegetation. Foody *et al.,* (2001) study supported our results according to which there is poor relationship between NDVI and biomass. Main problem is saturation due to which accuracy is less. The saturation can be due to mature crop or it may also be due to complex structure of forest in result of which broadband VIs didn't observe the biomass increase. This was actually in the case when vegetation or leaves completely cover the area so biomass was increase while the value of spectral index remained constant.

MSR and AGB

The correlation between MSR extracted form Sentinel-2 image has been shown in Fig. 2b. The coefficient of correlation was 0.44 which showed that 44% of field data have been explained by the MSR model while 56% of the data are not explained by this model. However, the correlation of MSR with AGB was less (R^2=0.44) as compared to NDVI is greater than ARVI. The results show that higher forest density was found at the north parts of the study area. The Fig. 4b showed range of MSR between 0 and 18.73; the positive values (18.73 or less) showed vegetation cover while the less values show no or less vegetation. Wang *et al.* (2016)

studied that reason of saturation is the computation of indices through NIR and Red spectral band and the red band absorb electromagnetic radiation and remains constant while the canopy cover increases hence in result at 100% canopy cover red energy absorption reaches to peak. Also, the soil reflectance and topography have effect on biomass estimation using spectral indices therefore assessment of different spectral indices is very useful (Heiskanen, 2006).
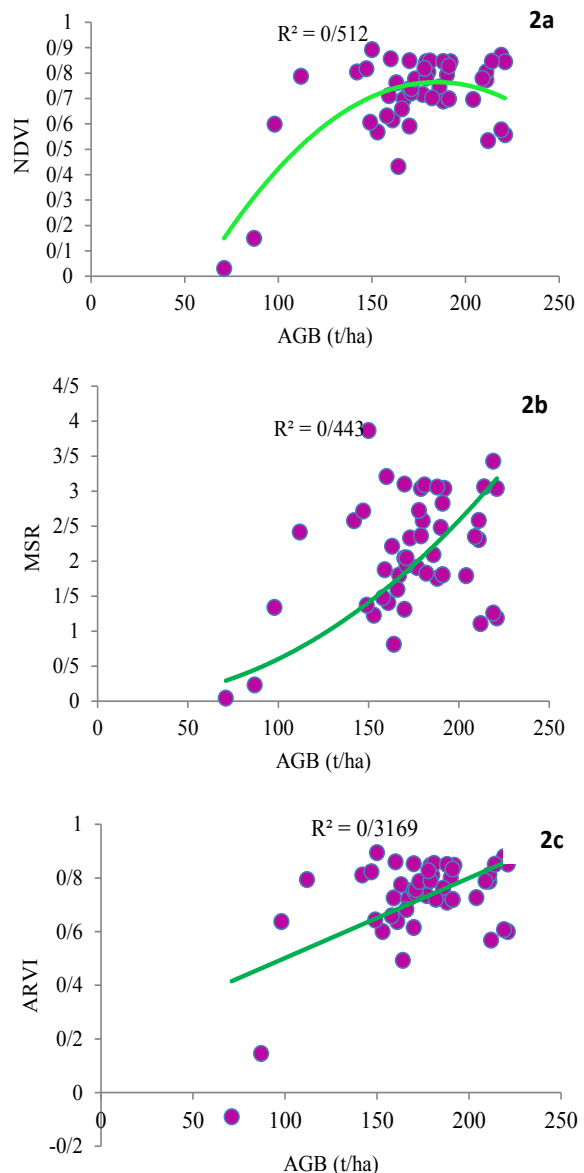
Fig. 2 (2a, 2b and 1c): Broadband spectral indices derived from sentinel-2 image

ARVI and AGB

The correlation between AGB values from field data and ARVI values derived has been shown in Fig. 2c. As pictured in the scatter plot, the coefficient of correlation was 0.31 which showed that relationship between ARVI and AGB is not too much strong as compared to rest of the indices (NDVI and MSR). The ARVI regression model can explain only 31% of variation in AGB data while 69 % of the data is not explained by this model. The Fig. 4c showed range of ARVI between -0.01 and 0.99; the positive values (0.99 or less) showed vegetation cover while the negative values shows less or no vegetation. The higher forest cover was mapped at northern part of the study area. While moving towards south west and south east there is comparatively less vegetation. In NIR portion of electromagnetic spectrum multiple scattering effect increases at 100% canopy cover resulting in inequality due to decrease in Red and increase in NIR band due to which biomass is poorly estimated (Mutanga and Skidmore, 2004).

Red-edge band vegetation indices
RENDVI-1 and AGB

The correlation between RENDVI-I and AGB values derived has been shown in Fig. 3a. The coefficient of correlation was 0.62 which showed that 62% of field data have been explained by the RENDVI-I model while 38% of the data are not explained by this model. However, the correlation of RENDVI-I with AGB was less (R^2=0.62) as compared to RENDVI2 yet greater than S2REP. The results show that forest density is found in all parts of the study area. The Fig. 5a showed range of RENDVI-I between -0.69 and 0; the positive values (0 or less) showed vegetation cover while the negative values show no or less vegetation. The reflectance of red portion is less while that of NIR and red-edge region is high. Our results of red-edge band spectral indices are validated by Mutanga *et al.* (2012) who reported that RENDVI have R^2 value of 0.67 while the NDVI R^2 value (0.39) was less. Also the spatial resolution have effect on the spectral indices performance the higher the spatial resolution higher will be accuracy and vice versa (Gara *et al.,* 2017). When the structure of forest is simple so there will be less saturation effect as compared to the forest having complex structure. From results it is concluded that red edge spectral indices should be used in mature and dense forest where saturation is normal problem using red band (Huete *et al.,* 2002).
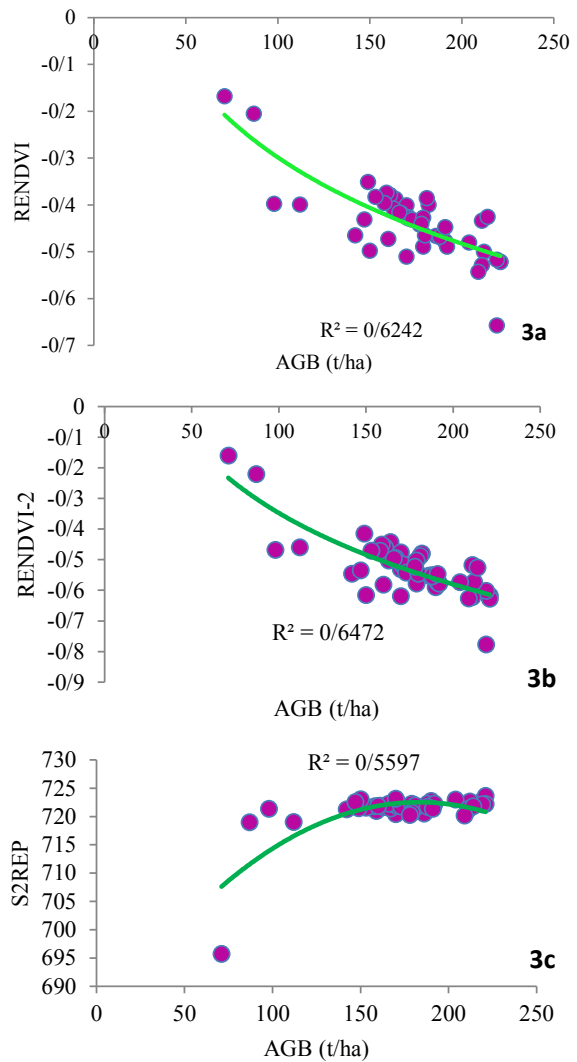

Fig. 3 (3a, 3b, and 3c): RE band based spectral indices derived from sentinel-2 image

RENDVI-II and AGB

The Fig. 3b showed the scatter plot between AGB values from field data and RENDVI-II values derived from image. The coefficient of correlation was 0.64 which mean that 64% of field data have been explained by the RENDVI-II based model while 36% of the data are not explained by this model. However, RENDVI-II is a proxy data and this much coefficient of correlation is considered good. The correlation of RENDVI-II was greater than (RENDVI-I and S2REP) and showed that higher forest density was observed in most of study area (Fig. 5b.). The Fig. 5b showed range of RENDVI2
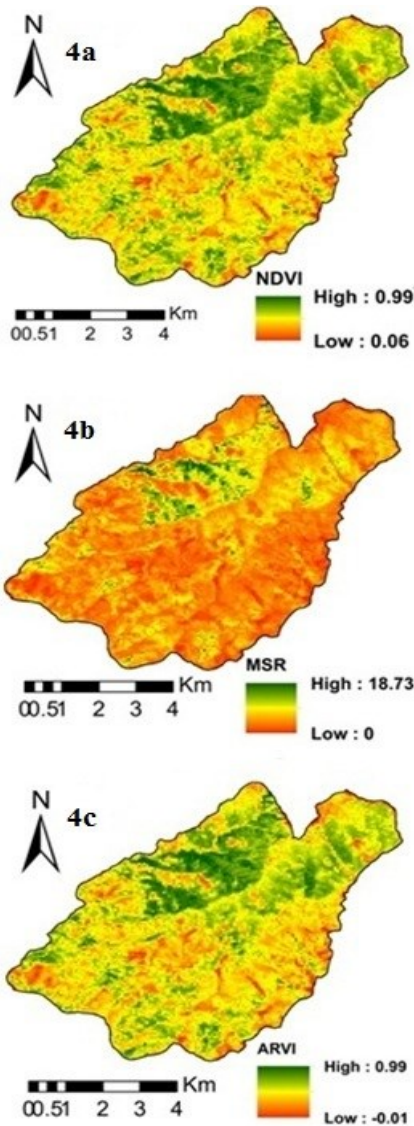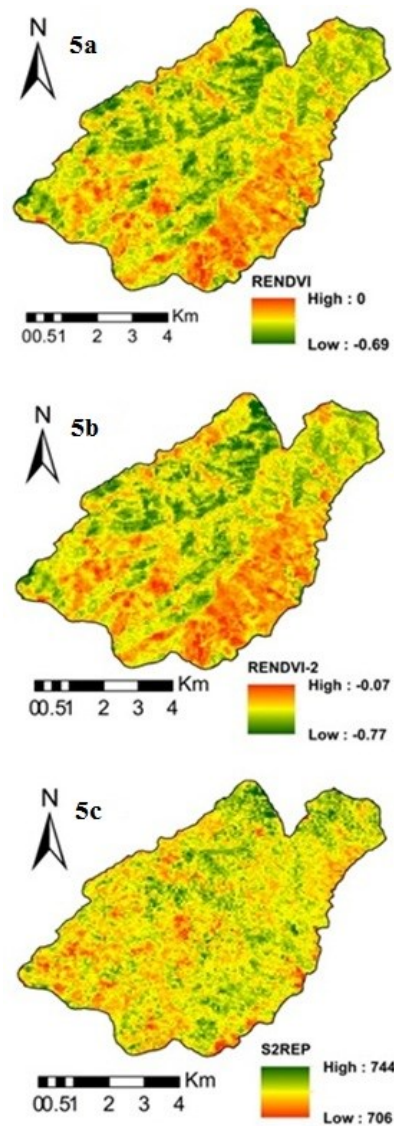
Fig. 4 (a, b, c): Broadband spectral indices

Fig. 5 (a, b, c): RE spectral indices

between -0.77 and -0.07; the positive values (-0.07 or less) showed vegetation cover while the -0.077 values show no or less vegetation. The relationships between these were best and high than broadband vegetation indices. RENDVI-2 had highest R^2 value of 0.64 while its RMSE was lowest (31.29 t/ha). The relationship of biomass with these vegetation indices is best due to the reason that red-edge band is located in high chlorophyll reflectance and absorption area which is between red and NIR region due to which the change in chlorophyll as well as leaf properties have greater effect on the red-edge spectral band (Slonecker *et al.,* 2009). It was found that red edge indices have more accuracy and correlation as compared to broadband indices (Xie *et al.,* 2018).

S2REP and AGB

The correlation between AGB values from field data and S2REP values derived has been shown in Fig. 3c. As the scatter plot depicted, the coefficient of correlation was 0.55 which showed that relationship between S2REP and AGB is not too much strong

as compared to rest of the RE indices. The S2REP regression model can explain only 55% of variation in AGB data while 45 % of the data is not explained by this model. The Fig. 5c showed range of S2REP between 706 and 744; the positive values (744 or less) showed vegetation cover while the second values shows less or no vegetation. The Fig. 5c showed that forest density is scattered in all area and was found at all part of the model except the south-east part of the model which shows comparatively less vegetation. In order to evaluate the performance of spectral indices using Red-edge, NIR and Red spectral bands various studies have been conducted (Chen *et al.,* 2007; Zhao *et al.,* 2007). From these studies it can be concluded that using red-edge spectral band

improves the accuracy of biomass estimation as the R^2 value increases with it. Chang and Shoshany (2016) explored that RE band indices for green biomass and RE indices showed excellent performance as compared broadband indices; R^2 of 0.94, 0.84 and 0.70 were observed for NDVIrededge, CIrededge and S2REP, respectively.

Stepwise regression model and AGB prediction

Results from stepwise linear regression have been shown in Table 3. All indices computed indices both barodband and narrowband (NDVI, MSR, ARVI, RENDVI, RENDVI-2, S2REP) were used are explanatory variables in stepwise method. The final model selected explanatory variables based on significance level as probability to

Table 2: Summary of regression models for sentinel-2 as spectral indices

Indices	Equation	R^2	SE	F	P-value
	Broadband spectral indices				
NDVI	Y= 104.84*NDVI+ 99.44	0.51	27.90	18.55	8.36E-05
ARVI	Y= 106.24*ARVI+ 97.12	0.31	27.23	21.80	2.55E-05
MSR	Y= 15.93*MSR+ 140.14	0.44	30.28	8.64	0.00507
	Red-edge band spectral indices				
RENDVI	Y= -334.4*RENDVI+ 26.81	0.62	20.57	73.50	3.6E-11
RENDVI-2	Y= -269.3*RENDVI2+ 32.16	0.64	20.59	73.36	3.7E-11
S2REP	Y= 4.62*S2REP -3162.8	0.55	27.67	19.63	5.57E-05

Table 3: Stepwise regression model and AGB prediction

Variables entered/ removed[a]			Model summary				
Variables Entered	Variables Removed	Significance	R	R square	Adjusted R Square	SE of the estimate	
RENDVI		0.000	.781[a]	.610	.602	20.579	
	NDVI	0.794			ANOVA		
	ARVI	0.950		Sum of Squares	df	Mean square	F
	MSR	0.257	Regression	31131.112	1	31131.112	73.508
	RENDVI2	0.525	Residual	19904.847	47	423.507	
	S2REP	0.356	Total	51035.959	48		

Coefficients						
	Unstandardized coefficients		Standardized coefficients	t	Sig.	Model equation
	B	S.E.				
(Constant)	26.814	17.394		1.542	.130	AGB= 26.81-334.4*RENDVI
RENDVI	-334.405	39.004	-.781	-8.574	.000	

a. Dependent variable: AGB
a. Predictors in the model: (Constant), RENDVI
Stepwise (Criteria: Probability-of-F-to-enter <= .050, Probability-of-F-to-remove >= .100).

Table 4: Accuracy assessment of regression models

Index type	Independent variable	Model	R^2	RMSE (t/ha)
Broadband indices	NDVI	AGB= 104.84*NDVI+ 99.44	0.51	53.82
Narrowband indices	RENDVI-2	AGB=-269.3*RENDVI2+ 32.16	0.64	31.29
All indices (Stepwise method)	RENDVI	AGB= 26.81-334.4*RENDVI	0.61	34.38

be selected was <= 0.05 and probability for exclusion was >= 0.100. As depicted in Table 3, the final model showed that only RENDVI was selected as explanatory variable while the rest of the indices (NDVI, MSR, ARVI, RENDVI-2 and S2REP) were not excluded because their significance value is higher than pre-defined threshold in the model. The overall coefficient of determination was 0.61 while, adjusted correlation was 0.60 with error estimate of 20.57 (t/ha) of AGB.

Accuracy assessment and biomass mapping

Three models (best broadband, best narrowband and stepwise selection) were selected for AGB prediction based on their performance (R^2 values) but among these three models, the best model was selected through by root mean square error (RMSE). The final model of RENDVI-2 has the lowest RMSE of 31.29 (t/ha) followed by the RENDVI stepwise model with RMSE of 34.38 (t/ha). The highest RMSE (53.82 t/ha) was determined for NDVI broadband model that why it was not selected for AGB estimation. RMSE evaluation showed that RENDVI-2 should be used to map spatial distribution of AGB over Muzafferabad area. The resultant map was shown in Fig. 6. From results it can be seen that density of forest is higher at northern part of study area since have higher biomass while moving towards south west and south east side vegetation is less resulting in lower biomass. The northern aspect is cool hence have more vegetation cover and biomass as compare to southern aspect which is warmer. The biomass of broadleaved species will be less while as compared to coniferous species due to low wood density, volume and age of broadleaved species than that of coniferous species. Young trees will have low biomass while old trees biomass will be high as biomass depends on tree age.

CONCLUSION

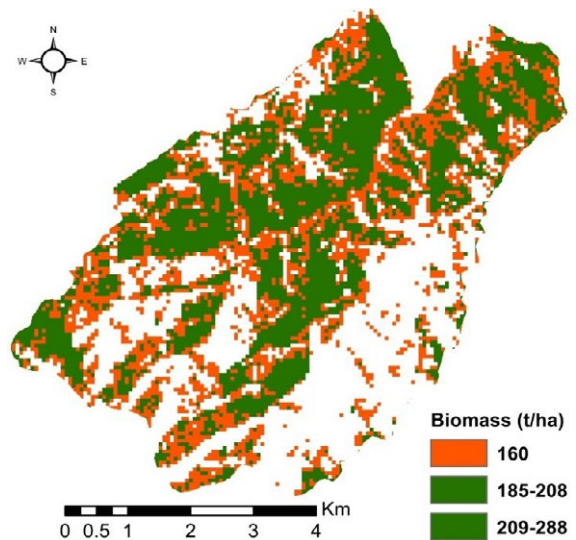This present explored Sentinel-2 imagery for estimation of above ground biomass. The study

Fig. 6: Biomass mapping using Sentinel-2 RE bands

primarily focused on comparison of broadband and narrowband indices derived from Sentinel-2 imagery. Broadband indices include normalized difference vegetation index, modified simple ratio and atmospherically resistant VI. Whereas red-edge band indices include RENDVI-1, RENDVI-II and sentinel-2 RE position. The findings reveals that the performance of Red-edge band spectral indices (RENDVI, RENDVI-2, S2REP) are good as compared to broadband spectral indices (NDVI, ARVI, MSR) in which RENDVI-2 performed better having R^2 value of 0.64. Results indicated that AGB can be accurately estimated from indices calculated from the wavelengths located in red edge of Sentinel-2. On the other, NDVI, MSR and ARVI have low AGB predictive performance. The results also showed that AGB density was sensitive to broadband indices due to saturation issues while narrowband have overcome this saturation issue in high forest density areas. These results further demonstrate that the sentinel-2 red edge band indices have the powerful potential to

estimate AGB efficiently compare to standard NDVI or other broadband indices. Further, it was found that there are still very few studies in Pakistan (and in the regions) dedicated to utilize Sentinel-2 data for estimating forest AGB. It is further research focusing on the Red Edge Bands of Sentinel-2 to estimate forest AGB should contribute to the regional estimates of carbon emissions and will assist the measurement, reporting and verification of reducing emissions from deforestation and forest degradation activities and annual development program "Carbon Stock Assessment of Forests of Khyber Pakthtunkhwa, Pakistan. The present study also assists forest manager during the implementation of pilot project through participatory management involving forest communities. The potential pilot project will not only generate income but also green employment. The link of the natural regeneration, reforestation, agroforestry and quantification by Sentinel-2 images for emission reduction will be beneficial for their livelihood. At larger scales, the participatory management reflects positive approach towards climate change mitigation and adaptation.

ACKNOWLEDGMENT

CONFLICT OF INTEREST

The author declares that there is no conflict of interests regarding the publication of this manuscript. In addition, the ethical issues, including plagiarism, informed consent, misconduct, data fabrication and/or falsification, double publication and/or submission, and redundancy have been completely observed by the authors.

ABBREVIATIONS

%	Percentage
°C	Degrees Celsius
AGB	Above ground biomass
B	Band
ARVI	Atmospherically resistant vegetation index
BEF	Biomass expansion factor
BOA	Bottom-of-atmospheric
BWD	Basic wood density
DBH	Diameter at breast height
df	Degree of freedom
DOS	Dark object subtraction
ERRA	Earthquake reconstruction and rehabilitation authority
ESA	European space agency
F	Fisher value
ha	Hectare
kg/m^3	Kilogram per cubic meter
L1C	Level-1C
m	Meter
m^3	Cubic meter
MSR	Modified simple ratio
N	North
NIR	Near infrared
nm	Nanometer
P-value	Significance value
R	RED
R^2	Coefficient of Correlation
RVI	Ratio Vegetation Index
RE	Red-edge
REIP	Red-Edge Inflation Point
RENDVI-1	Red Edge normalized difference vegetation index -1
RENDVI-2	Red edge normalized difference vegetation index -2
RMSE	Root mean square error
RS	Remote sensing
S2REP	Sentinel-2 red-edge position
SE	Standard error
Sen2Cor	Sentinel-2 correction
SNAP	Sentinel application toolbox
SWIR	Short wave infrared
t	Ton
T	T-value
TOA	Top-of-atmosphere
UTM	Universal transverse Mercator
V	Volume
VIs	Vegetation indices
WGS	World geodetic system

REFERENCES

Adan, M.S. (2017). Integrating Sentinel-2A derived indices and terrestrial laser scanner to estimate above ground biomass/carbon in Ayer Hitam tropical forest, Malaysia, Master of Science, University of Twente, The Netherlands.

Adam, E.; Mutanga, O.; Rugege, D., (2010). Multispectral and hyperspectral remote sensing for identification and mapping of wetland vegetation: a review. Wetland Ecol. Manage., 18(3): 281-296 **(16 pages).**

Ahmad, A.; Mirza, S. N.; Nizami, S.M., (2014). Assessment of biomass and carbon stocks in coniferous forest of Dir Kohistan, KPK. Pak. J. Agric. Sci., 51(2): 335-350 **(16 pages)**.

Ali, A.; Ullah, S.; Bushra, S.; Ahmad, N.; Ali, A.; Khan, M.A., (2018). Quantifying forest carbon stocks by integrating satellite images and forest inventory data. Aust. J. For. Sci., 135 (2): 93–117 **(25 pages)**.

Asadzadeh, S.; de Souza Filho, C.R., (2016). Investigating the capability of worldview-3 superspectral data for direct hydrocarbon detection. Remote Sens. Environ. 173: 162–173 **(12 pages)**.

Calvão, T.; Palmeirim, J.M., (2011). A comparative evaluation of spectral vegetation indices for the estimation of biophysical characteristics of Mediterranean semi-deciduous shrub communities. Int. J. Remote Sens., 32(8): 2275-2296 **(22 pages)**.

Chang, J.; Shoshany, M., (2016). Red-edge ratio Normalized Vegetation Index for remote estimation of green biomass. In 2016 IEEE International Geoscience and Remote Sensing Symposium (IGARSS), 1337-1339 **(3 pages).**

Chen, J.-C.; Yang, C.-M.; Wu, S.-T.; Chung, Y.-L.; Charles, A. L.; Chen, C.-T., (2007). Leaf chlorophyll content and surface spectral reflectance of tree species along a terrain gradient in Taiwan's Kenting National Park. Stud, 48: 71-77 **(7 pages)**.

Chen, J. M., (1996). Evaluation of vegetation indices and a modified simple ratio for boreal applications. Canad J Remot Sens., 22(3): 229-242 **(14 pages)**.

Cho, M.A.; Skidmore, A.K., (2006). A new technique for extracting the red edge position from hyperspectral data: The linear extrapolation method. Remote Sens. Environ., 101: 181–193 **(13 pages)**.

Cho, M.A.; Skidmore, A.K.; Atzberger, C., (2008). Towards red-edge positions less sensitive to canopy biophysical parameters for leaf chlorophyll estimation using properties optique spectrales des feuilles (prospect) and scattering by arbitrarily inclined leaves (sailh) simulated data. Int. J. Remote Sens., 29: 2241–2255 **(14 pages)**.

Chrysafis, I.; Mallinis, G.; Siachalou, S.; Patias, P., (2017). Assessing the relationships between growing stock volume and Sentinel-2 imagery in a mediterranean forest ecosystem. Remote Sens Lett., 8(6): 508-517 **(10 pages).**

Clevers, J.G.W.; Gitelson, A.A., (2013). Remote estimation of crop and grass chlorophyll and nitrogen content using red-edge bands on sentinel-2 and -3. Int. J. Appl. Earth Obs. Geoinf., 23: 344–351 **(8 Pages).**

Delegido, J.; Verrelst, J.; Meza, C.M.; Rivera, J.P.; Alonso, L.; Moreno, J., (2013). A red-edge spectral index for remote sensing estimation of green LAI over agroecosystems. Eur. J. Agron., 46: 42–52 **(11 pages).**

ERRA, (2007). Muzaffarabad Earthquake Reconstruction and Rehabilitation Authority. District Profile. Prime Minister's Secretariat, Islamabad, Kamran Printers, Blue Area., 1-3 **(3 pages).**

Drusch, M.; Del Bello, U.; Carlier, S.; Colin, O.; Fernandez, V.; Gascon, F.; Hoersch, B.; Isola, C.; Laberinti, P.; Martimort, P., (2012). Sentinel-2: Esa's optical high-resolution mission for gmes operational services. Remote Sens. Environ., 120: 25–36 **(12 pages)**.

Dusseux, P.; Hubert-Moy, L.; Corpetti, T.; Vertès, F., (2015). Evaluation of Spot imagery for the estimation of grassland biomass. Int. J. Appl. Earth Obs. Geoinf., 38: 72-77 **(6 pages)**.

Egbers, R., (2016). Sentinel-2 data processing and identifying glacial features in Sentinel-2 imagery, TU Delft, University of Technology, The Netherlands.

Foody, G.M.; Cutler, M.E.; Mcmorrow, J.; Pelz, D.; Tangki, H.; Boyd, D.S.; Douglas, I., (2001). Mapping the biomass of Bornean tropical rain forest from remotely sensed data. Global Ecol. Biogeogr., 10(4): 379-387 **(9 pages)**.

Frampton, W.J.; Dash, J.; Watmough, G.; Milton, E.J., (2013). Evaluating the capabilities of Sentinel-2 for quantitative estimation of biophysical variables in vegetation. ISPRS J. Photogramm. Remote Sens., 82: 83–92 **(10 pages)**.

Fukuda, M.; Lehara, T.; Matsumoto, M., (2003). Carbon stock estimates for sugi and hinoki forests in Japan. Forest Ecol. Manage., 184(1): 1-6 **(6 pages)**.

Gara, T.W.; Murwira, A.; Dube, T.; Sibanda, M.; Rwasoka, D.T.; Ndaimani, H.; Hatendi, C.M., (2017). Estimating forest carbon stocks in tropical dry forests of Zimbabwe: exploring the performance of high and medium spatial-resolution multispectral sensors. Southern For. J. For. Sci., 79(1): 31-40 **(9 pages)**.

Gascon, F.; Berger, M., (2007). GMES Sentinel-2 mission requirements document. Rapport technique, ESA.

Gholizadeh, A.; Mišurec, J.; Kopačková, V.; Mielke, C.; Rogass, C., (2016). Assessment of red-edge position extraction techniques: A case study for norway spruce forests using hymap and simulated sentinel-2 data. Forests., 7(10): 226-242 **(17 pages)**.

Heiskanen, J. (2006). Estimating aboveground tree biomass and leaf area index in a mountain birch forest using ASTER satellite data. Int. J. Remote Sens., 27(6): 1135-1158 **(24 pages)**.

Huete, A.; Didan, K.; Miura, T.; Rodriguez, E. P.; Gao, X.; Ferreira, L. G., (2002). Overview of the radiometric and biophysical performance of the MODIS vegetation indices. Remote Sens. Environ., 83(1-2): 195-213 **(19 pages).**

Kaufman, Y.J.; Tanre, D., (1992). Atmospherically resistant vegetation index (ARVI) for EOS-MODIS. IEEE Trans Geosci Remot Sens., 30(2):261-270 **(10 pages).**

Karakoç, A.; Karabulut, M., (2019). Ratio-Based vegetation indices for biomass estimation depending on grassland characteristics. Turk. J. Bot., 43: 619-633 **(15 pages)**.

Karlson, M.; Ostwald, M.; Reese, H.; Bazié, H.R.; Tankoano, B., (2016). Assessing the potential of multi-seasonal worldview-2 imagery for mapping West African agroforestry tree species. Int. J. Appl. Earth Obs. Geoinf., 50: 80–88 **(9 pages)**.

Kross, A.; McNairn, H.; Lapen, D.; Sunohara, M.; Champagne, C., (2015). Assessment of rapideye vegetation indices for estimation of leaf area index and biomass in corn and soybean crops. Int. J. Appl. Earth Obs. Geoinf., 34: 235–248 **(14 pages)**.

May, A.M.B.; Pinder, J.E.; Kroh, G.C., (2010). A comparison of Landsat Thematic Mapper and SPOT multi-spectral imagery for the classification of shrub and meadow vegetation in northern California, U.S.A. Int. J. Remote Sens., 18 (18): 3719-3728 **(10 pages)**.

Martins, V.S.; Barbosa, C.C.; de Carvalho, L.A.; Jorge, D.S.; Lobo, F.D.; Novo, E.M., (2017). Assessment of atmospheric correction methods for Sentinel-2 msi images applied to Amazon floodplain lakes. Remote Sens., 9(4): 322-340 **(19 pages)**.

Mohren, G.M.J.; Hasenauer, H.; Köhl, M.; Nabuurs, G.J., (2012).

Forest inventories for carbon change assessments. Curr. Opin. Environ. Sustainable. 4(6): 686-695 **(10 pages)**.

Molto, Q.; Rossi, V.; Blanc, L. (2013). Error propagation in biomass estimation in tropical forests. Methods Ecol. Evol., 4(2): 175-183 **(9 pages)**.

Mundava, C.; Helmholtz, P.; Schut, A.G.T.; Stovold, R.; Corner, R., (2014). Evaluation of vegetation indices for rangeland biomass estimation in the kimberley area of western Australia. ISPRS Ann Photogram. Remote Sens Spat. Inf. Sci., 2(7): 47-53 **(17 pages)**.

Mutanga, O.; Skidmore, A.K., (2004a). Hyperspectral band depth analysis for a better estimation of grass biomass (Cenchrus ciliaris) measured under controlled laboratory conditions. Int. J. Appl. Earth Obs. Geoinf., 5(2): 87-96 **(10 pages)**.

Mutanga, O.; Adam, E.; Cho, M.A., (2012). High density biomass estimation for wetland vegetation using WorldView-2 imagery and random forest regression algorithm. Int. J. Appl. Earth Obs. Geoinf., 18: 399-406 **(8 pages)**.

Paustian, K.; Ravindranath, N. H.; van Amstel, A. R., (2006). IPCC guidelines for national greenhouse gas inventories. No. Part 2.

Richter, K.; Hank, T.B.; Vuolo, F.; Mauser, W.; D'Urso, G., (2012). Optimal exploitation of the Sentinel-2 spectral capabilities for crop leaf area index mapping. Remote Sens., 4: 561–582 **(22 pages)**.

Louis, J.; Debaecker, V.; Pflug, B.; Main-Knorn, M.; Bieniarz, J.; Mueller-Wilm, U.; Cadau, E.; Gascon, F., (2016). Sentinel-2 Sen2Cor: L2A processor for users. InProceedings Living Planet Symposium 2016, Spacebooks Online. 1-8 **(8 pages)**.

Rouse, J.W.; Haas, R.H.; Schell, J.A.; Deering, D.W., (1973). Monitoring vegetation systems in the Great Plains with ERTS. In: Third ERTS Symposium. NASA, 309–317 **(9 pages)**.

Roy, D.P.; Li, J.; Zhang, H.K.; Yan, L., (2016). Best practices for the reprojection and resampling of Sentinel-2 multi spectral instrument level 1C data. Remote Sens. Lett., 7(11): 1023-1032 **(10 pages)**.

Shaheen, H.; Khan, R. W. A.; Hussain, K.; Ullah, T. S.; Nasir, M.; Mehmood, A., (2016). Carbon stocks assessment in subtropical forest types of Kashmir Himalayas. Pak. J. Bot., 48(6): 2351-2357 **(7 pages)**.

Schoene, D., (2002). Terminology in assessing and reporting forest carbon change. In second expert meeting on harmonizing forest-related definitions for use by various stakeholders. FAO, Rome.

Slonecker, T.; Haack, B.; Price, S., (2009). Spectroscopic analysis of arsenic uptake in Pteris ferns. Remote Sens, 1(4): 644-675 **(31 pages)**.

Verrelst, J.; Munoz, J.; Alonso, L.; Delegido, J.; Rivera, J.P.; Camps-Valls, G.; Moreno, J. (2012). Machine learning regression algorithms for biophysical parameter retrieval: Opportunities for Sentinel-2 and -3. Remote Sens. Environ., 118: 127–139 **(12 pages)**.

Wang, C.; Feng, M.-C.; Yang, W.-D.; Ding, G.-W.; Sun, H.; Liang, Z.-Y.; Qiao, X.X., (2016). Impact of spectral saturation on leaf area index and aboveground biomass estimation of winter wheat. Spectroscopy. Lett., 49(4): 241-248 **(8 pages)**.

Wang, J.; Liu, Z.; Yu, H.; Li, F., (2017). Mapping spartina alterniflora biomass using LiDAR and hyperspectral data. Remote Sens., 9(6): 589-601 **(13 pages)**.

Xie, Q.; Dash, J.; Huang, W.; Peng, D.; Qin, Q.; Mortimer, H.; Casa, R.; Pignatti, S.; Laneve, G.; Pascucci, S.; Dong, Y., (2018). Vegetation indices combining the red and red-edge spectral information for leaf area index retrieval. IEEE J Top App Ear Obser Remot Sens., 11(5): 1482-1493 **(12 pages)**.

Zhao, D.; Huang, L.; Li, J.; Qi, J., (2007). A comparative analysis of broadband and narrowband derived vegetation indices in predicting LAI and CCD of a cotton canopy. ISPRS J. Photogramm Remote Sens., 62(1): 25-33 **(9 Pages)**.

AUTHOR (S) BIOSKETCHES

Imran, A.B., B.Sc., Department of Forestry and Range Management, PMAS Arid Agriculture University, Rawalpindi, Pakistan. Email: *areebaimran1996@yahoo.com*

Khan, K., M.Sc., Instructor, Institute of Environmental Science and Engineering, National University of Science and Technology, Pakistan. Email: *naveed.iese.nust@gmail.com*

Ali, N., M.Sc., Department of Forestry and Wildlife Management, University of Haripur, Pakistan. Email: *foresternizar@gmail.com*

Ahmad, N., M.Sc., Instructor, Sub-Divisional Wildlife Officer, Ministry of Forestry, Environment and Wildlife, Khyber Pukhtunkhwa, Pakistan. Email: *naveedahmad795@gmail.com*

Ali, A., M.Sc., Deputy Ranger Wildlife, Ministry of Forestry, Environment and Wildlife, Khyber Pukhtunkhwa, Pakistan. Email: *aamirb4u68@yahoo.com*

Shah, K., M.Sc., Sub-Divisional Wildlife Officer, Ministry of Forestry, Environment and Wildlife, Khyber Pukhtunkhwa, Pakistan. Email: *kiramatshah4@gmail.com*